processes

Article

Research on Segmented Belt Acceleration Curve Based on Automated Mechanical Transmission

Yunxia Li [1,2,*] and Lei Li [1,2]

[1] School of Mechanical & Automotive Engineering, Qilu University of Technology (Shandong Academy of Sciences), Jinan 250353, China; lilei9lily@163.com
[2] Shandong Institute of Mechanical Design and Research, Jinan 250353, China
* Correspondence: liyunxia@qlu.edu.cn

Abstract: An automated mechanical transmission (AMT) is proposed as a new soft starter for medium-scale belt conveyors in this paper. The AMT is used to start the belt conveyor and shift gears step by step to make the belt conveyor accelerate softly. Based on analyzing common soft-starting acceleration curves, a segmented belt acceleration curve is proposed as a new soft-starting acceleration curve. By analyzing the AMT soft-starting system, the system modeling is built and the AMT output shaft's angular acceleration is proposed to be controlled to control the belt acceleration. The AMT soft-starting simulation model is established in the environment of AMESim, and simulation results of the soft-starting process from the first to eighth gear positions are given. The main parameter curves of the AMT soft-starting system including the belt, driving pulley, and AMT output shaft are analyzed. The simulation model can indicate the viscoelastic property of the belt. The simulation results prove that the segmented belt acceleration is appropriate for a medium-scale belt conveyor and provide a theoretical and reasonable basis for using an AMT as a soft starter.

Keywords: automated mechanical transmission; shift gear; soft starting; belt conveyor; segmented acceleration curve

check for updates

Citation: Li, Y.; Li, L. Research on Segmented Belt Acceleration Curve Based on Automated Mechanical Transmission. *Processes* **2022**, *10*, 106. https://doi.org/10.3390/pr10010106

Academic Editors: Liming Dai and Jialin Tian

Received: 4 September 2021
Accepted: 2 November 2021
Published: 5 January 2022

1. Introduction

Belt conveyors are important transport equipment for transmitting bulk materials. Compared with heavy-duty trucks and trains, belt conveyors have some specific advantages such as large transport capacity, continuous operation, and low transport costs. More than two million conveyors are in operation annually in the world. Belt conveyors with long distances and heavy loads are widely used in coal mines, metallurgical industries, and other industries where the use of trucks and trains is impractical [1–3]. Conveyor belts are made of rubber, steel wire, and fiber, which have some viscoelastic properties that give the belt conveyor complex dynamical characteristics. Serious accidents can take place during startup if the belt acceleration is too large for a belt conveyor with long distance and high power, such as slipping, tear, and severe wear [4–6]. Speed control of the belt conveyors has become the key point of the medium-scale belt conveyors during starting and stopping [7–11].

Soft-starting is required during startup for belt conveyors considering no slipping and no tearing. The belt speed curve should meet the requirements of less speed and less acceleration variation per unit time for the purpose of softness. Therefore, the parameters of belt speed and acceleration should be controlled by means of equipment. Using soft-starting equipment can realize the belt conveyor's soft starting. The soft-starting technologies are mainly AC variable frequency speed regulation technology and hydro-viscous variable speed regulation technology. For variable frequency speed regulation technology, the output speed of the three-phase asynchronous motor can be regulated by adjusting its frequency [12,13]. It requires clean surroundings and sufficient ventilation, leading to high maintenance costs. For hydro-viscous variable speed regulation technology, the output speed of the wet clutch can be regulated by adjusting hydraulic pressure [14,15]. Similarly, it also requires excellent cleanliness and good ventilation. Apparently, the above two soft-starting technologies cannot meet the requirements of dirty working conditions such as those in underground coal mines. In addition, their purchasing costs are very high. Thus, a soft-starting technology with low costs and high reliability is needed for the belt conveyors used in adverse environments such as underground coal mines.

In the last two decades, AMT has been widely used in heavy-duty vehicles for some advantages of large transmitted torque, high transmission efficiency, low purchasing costs, low maintenance costs, and longer service life [16–20]. The AMT has a high transmission efficiency of more than 90% [21,22], while other soft-starting technologies cannot provide such a high transmission efficiency. With continuous study and design, the input torque of the AMT supplied by ZF Friedrichshafen AG can reach 3400 N·m, which can meet the requirements of the transmitted torque for the heavy-duty vehicles and medium-scale belt conveyors with 500 kW. The author has published papers using AMT as a soft starter of the belt conveyors since 2013 [23,24]. The AMT soft-starting system for belt conveyors mainly contains a three-phase asynchronous motor, an AMT, a reducer, and a belt conveyor.

Researchers have done a great deal of theoretical and experimental studies on the soft-starting acceleration or speed curves in the past four decades, for the purpose of decreasing the belt acceleration and the belt jerk during starting. In 1983, Harrison proposed a sine acceleration curve for the belt conveyors and obtained an S-type belt speed curve [25,26]. In 1987, Nordell et al. proposed a triangular acceleration curve as a soft-starting acceleration curve for belt conveyors [27,28]. In 1994, Singh proposed a soft-starting acceleration curve with a creep section [29]. In 1998, Song proposed a trapezoidal acceleration curve as a soft-starting acceleration curve for belt conveyors [30]. In 2000, Bardos proposed a parabolic acceleration curve as a soft-starting acceleration curve for belt conveyors [31]. All those soft-starting acceleration curves can make the belt accelerate softly and result in the belt speed curve being S-shaped. Therefore, designing a soft-starting acceleration for an AMT as a soft starter is key in starting the medium-scale belt conveyors softly.

Given a belt acceleration, the needed AMT output shaft's angular acceleration can be calculated by driveline system parameters between the AMT and the conveyor. For the purpose of controlling the belt acceleration according to the designed curve, the AMT output shaft's angular acceleration should be controlled according to the corresponding belt acceleration curve. In practice, the speed sensors measuring the AMT input and output shafts can provide accurate information when the AMT is working. In addition, the angular acceleration of the AMT input and output shafts can be calculated by the speed sensors. Therefore, controlling the AMT output shaft's angular acceleration is possible. The paper provides a segmented belt acceleration curve for an AMT with many gears, which is a new belt acceleration curve in comparison with traditional belt acceleration curves.

The paper is organized as follows: In Section 2, a segmented acceleration curve is proposed for the AMT as a soft starter. In Section 3, the AMT soft starting system is described and the dynamic model is built. In Section 4, the simulation model of the AMT soft-starting system based on AMESim software is built and the simulation results are analyzed.

2. Segmented Belt Acceleration Curve

The expressions of the four soft-starting acceleration curves as mentioned above are analyzed below. By analyzing the characteristics of AMT, a new soft-starting acceleration curve suitable to start the belt conveyors for AMT as a soft starter is developed.

The sine acceleration and its jerk curves are expressed as Equation (1).

$$\begin{cases} a(t) = \frac{\pi}{2T} v_b \sin\left(\frac{\pi}{T} t\right) \\ j(t) = \frac{\pi^2}{2T^2} v_b \cos\left(\frac{\pi}{T} t\right) \end{cases} \quad (0 \le t \le T) \tag{1}$$

where t is the time, v_b is the belt target speed of the belt conveyor, T is the starting time of the belt conveyor, and $a(t)$ and $j(t)$ are the belt acceleration and the belt jerk.

The triangular acceleration and its jerk curves are expressed as Equation (2).

$$\begin{cases} a(t) = \begin{cases} 4v_b \frac{t}{T^2} & (0 \le t \le T/2) \\ 4v_b\left(\frac{1}{T} - \frac{t}{T^2}\right) & (T/2 < t \le T) \end{cases} \\ j(t) = \begin{cases} 4v_b \frac{1}{T^2} & (0 \le t \le T/2) \\ -4v_b \frac{1}{T^2} & (T/2 < t \le T) \end{cases} \end{cases} \quad (2)$$

The trapezoidal acceleration and its jerk curves are expressed as Equation (3).

$$\begin{cases} a(t) = \begin{cases} \frac{N^2 v_b}{(N-1)T^2} t & (0 \le t \le t_s) \\ \frac{N v_b}{(N-1)T} & (t_s < t < T - t_s) \\ \frac{N^2 v_b}{(N-1)T^2}(T-t) & (T - t_s \le t \le T) \end{cases} \\ j(t) = \begin{cases} \frac{N^2 v_b}{(N-1)T^2} & (0 \le t \le t_s) \\ 0 & (t_s < t < T - t_s) \\ -\frac{N^2 v_b}{(N-1)T^2} & (T - t_s \le t \le T) \end{cases} \end{cases} \quad (3)$$

where N is a natural number greater than or equal to 4 and t_s is the ascent or descent acceleration stage of the trapezoidal acceleration curve expressed as $t_s = T/N$.

The parabolic acceleration and its jerk curves are expressed as Equation (4).

$$\begin{cases} a(t) = 6v_b\left(\frac{t}{T^2} - \frac{t^2}{T^3}\right) \\ j(t) = 6v_b\left(\frac{1}{T^2} - 2\frac{t}{T^3}\right) \end{cases} (0 \le t \le T) \quad (4)$$

Under the conditions of the same starting time and same belt target speed, the above four soft-starting accelerations and their jerk curves are presented in Figure 1. Figure 1a gives the comparison results from the changes of the acceleration curves, and Figure 1b gives the comparison results from the changes of the jerk curves.

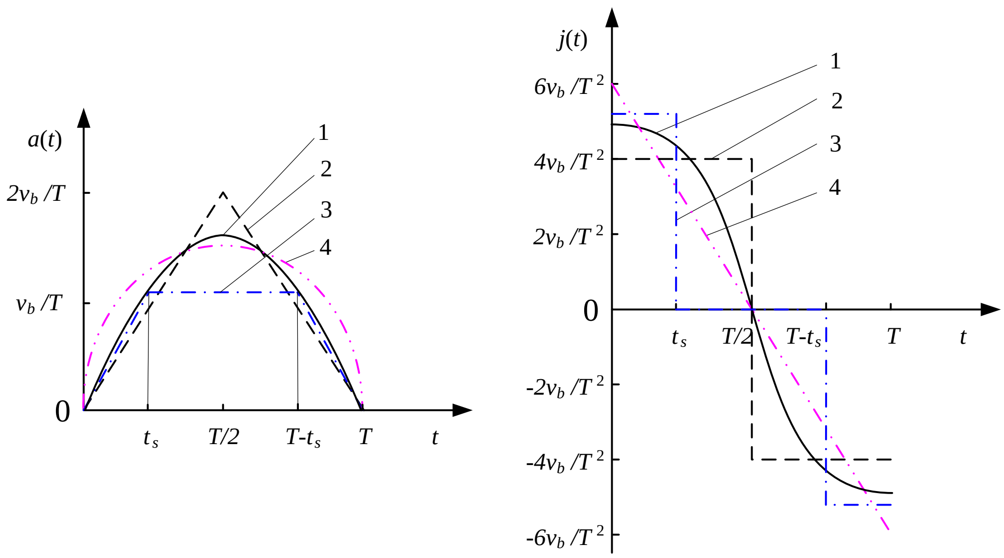

(**a**) acceleration curves (**b**) jerk curves

Figure 1. Comparisons of four soft-starting curves: 1-sine acceleration; 2-triangular acceleration; 3-trapezoidal acceleration; 4-parabolic acceleration.

When N is greater than or equal to 4, ranking the maximum values of the belt acceleration from large to small, triangular acceleration, sine acceleration, parabolic acceleration, and trapezoidal acceleration curves occupy the first, second, third, and last places, respectively. When N is equal to 4, ranking the maximum value of the belt jerk from large to small, parabolic acceleration, trapezoidal acceleration, sine acceleration, and triangular acceleration curves occupy the first, second, third, and last places, respectively. When N is greater than 4, ranking the maximum values of the belt jerk from large to small, trapezoidal acceleration, parabolic acceleration, sine acceleration, and triangular acceleration curves occupy the first, second, third, and last places, respectively. Among the jerk curves, the triangular acceleration and trapezoidal acceleration curves have sudden change phenomena. From the perspective of control difficulties, the sine acceleration and parabolic acceleration curves are complicated to control, making their acceleration algorithms more complex than those of the other two soft-starting acceleration curves.

The above soft-starting acceleration curves can effectively control the AC variable frequency motor and the hydro-viscous start transmission. An AMT as a soft starter needs to upshift gradually to accelerate the belt, and the above four soft-starting acceleration curves cannot directly be used. Power needs to be cut using the clutch during upshifting, and the soft-starting acceleration curve should be considered in this situation. The transmitted torque of the clutch is related to the force of the diaphragm spring, and its value is a third-order polynomial related to the big end displacement of the diaphragm [32,33]. While the automatic clutch actuator is equipped to control the small end displacement of the diaphragm spring through thrust bearing, the big end displacement of the diaphragm spring can be controlled on account of the lever principle. Thus, the belt acceleration can be controlled by the transmitted torque of the clutch, which can be controlled by the clutch actuator. Considering the complexity of the shifting control and the clutch control, the algorithm of the belt acceleration should not be too complicated. Therefore, the soft-starting acceleration curve should be designed practically.

The clutch should be first disengaged for shifting and be engaged finally after shifting, and the power flow is interrupted during this interval. Thus, the belt cannot be accelerated during shifting. As can be seen from Figure 1, the maximum value of the trapezoidal acceleration curve is lower than the maximum values of the other three soft-starting curves under the condition of the same starting time. In addition, the horizontal line of the trapezoidal acceleration curve lowers control difficulty for the clutch. Therefore, to minimize the belt acceleration and belt jerk, the trapezoidal acceleration curve is chosen as the basic acceleration curve and N is set equal to 4. A segmented acceleration curve is proposed for an AMT as a soft starter based on the above analysis, as shown in Figure 2.

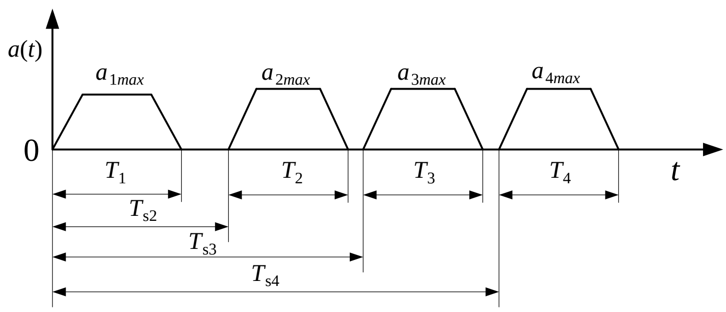

Figure 2. Starting acceleration curve for AMT.

The segmented acceleration curve includes several trapezoidal acceleration curves determined by the maximum running speed, motor rated speed, and gear positions. T_1, T_2, T_3, and T_4 are the acceleration times for the respective gear positions. a_{max1}, a_{max2}, a_{max3}, and a_{max4} are designed maximum accelerations under the conditions of first gear, second gear, third gear, and fourth gear, respectively. T_{s2}, T_{s3}, and T_{s4} are starting times for accelerations under second, third, and fourth gear positions. For the purpose of stretching the whole belt, the belt is kept running for longer than 5 s after the acceleration stage labeled T_1 under first gear is completed. Owing to the belt being too long, the end of the conveyor end runs behind the head of the conveyor head during the acceleration process. That is to say, the time difference value between T_{s2} and T_1 contains 5 s and shifting time for second gear. The belt is kept running for more than 2 s for the purpose of making up the speed loss between the belt head and the belt end after the acceleration stage is completed under second gear or higher gear. Then, the AMT is shifted to another higher gear position. In this way, the upshifting operation should be completed until the designed target belt speed is reached and the soft-starting process of the belt conveyor is finished. Generally, more than five gear positions are provided by a heavy-duty AMT, which can meet the needs for belt speed.

The segmented acceleration curve for a conveyor belt is expressed as Equation (5).

$$\begin{cases} a(t) = \begin{cases} \frac{4a_{1max}}{T_1}t & \left(0 \le t \le \frac{1}{4}T_1\right) \\ a_{1max} & \left(\frac{1}{4}T_1 < t < \frac{3}{4}T_1\right) \\ \frac{4a_{1max}}{T_1}(T_1 - t) & \left(\frac{3}{4}T_1 \le t \le T_1\right) \end{cases} \\ a(t) = \begin{cases} \frac{4a_{2max}}{T_2}(t - T_{s2}) & \left(T_{s2} \le t \le T_{s2} + \frac{1}{4}T_2\right) \\ a_{2max} & \left(T_{s2} + \frac{1}{4}T_2 < t < T_{s2} + \frac{3}{4}T_2\right) \\ \frac{4a_{2max}}{T_2}(T_{s2} + T_2 - t) & \left(T_{s2} + \frac{3}{4}T_2 \le t \le T_{s2} + T_2\right) \end{cases} \\ a(t) = \begin{cases} \frac{4a_{3max}}{T_3}(t - T_{s3}) & \left(T_{s3} \le t \le T_{s3} + \frac{1}{4}T_3\right) \\ a_{3max} & \left(T_{s3} + \frac{1}{4}T_3 < t < T_{s3} + \frac{3}{4}T_3\right) \\ \frac{4a_{3max}}{T_3}(T_{s3} + T_3 - t) & \left(T_{s3} + \frac{3}{4}T_3 \le t \le T_{s3} + T_3\right) \end{cases} \\ a(t) = \begin{cases} \frac{4a_{4max}}{T_4}(t - T_{s4}) & \left(T_{s4} \le t \le T_{s4} + \frac{1}{4}T_4\right) \\ a_{4max} & \left(T_{s4} + \frac{1}{4}T_4 < t < T_{s4} + \frac{3}{4}T_4\right) \\ \frac{4a_{4max}}{T_4}(T_{s4} + T_4 - t) & \left(T_{s4} + \frac{3}{4}T_4 \le t \le T_{s4} + T_4\right) \end{cases} \\ \cdots \end{cases} \tag{5}$$

3. System Description and Modeling

3.1. Soft-Starting System

Figure 3 shows the soft-starting driving system based on AMT. The soft-starting driving system mainly includes a three-phase induction motor, AMT, reducer, and belt conveyor. Powered by a three-phase induction motor, the transmitted torque is increased by AMT and reducer and drives the belt conveyor.

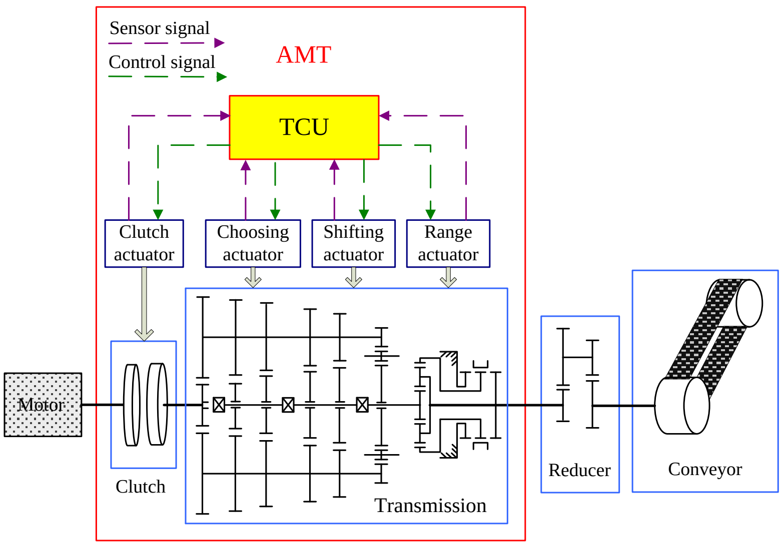

Figure 3. Soft-starting driving system.

AMT comprises transmission control unit (TCU), actuators, clutch, and transmission. The TCU controls the clutch engagement and disengagement through the clutch actuator, which is operated by high-speed on–off solenoid valves. The TCU controls shifting through the choosing actuator, shifting actuator, and range actuator. The range actuator is used to control two gear positions (low and high gear positions) of the auxiliary transmission box. The shifting actuator is used to control several gear positions of the main transmission box. Thus, more than 10 gear positions of the AMT can be obtained. The belt acceleration can be controlled according to the designed segmented acceleration curve by the TCU, and the soft-starting process of the belt conveyor is achieved.

3.2. AMT Driving Modeling

An AMT driving model for a soft-starting driving system can be built as shown in Figure 4.

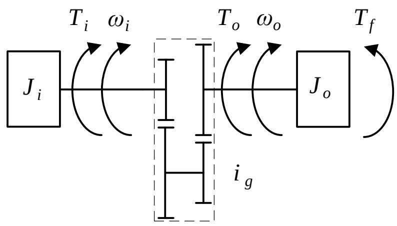

Figure 4. AMT driving model.

The parameters in Figure 4 are illustrated in Table 1.

Table 1. Model parameters.

Signal	Mean
J_i	AMT input shaft's moment of inertia
T_i	Transmml:mitted torque of the AMT input shaft
ω_i	AMT input shaft's speed
J_o	AMT output shaft's equivalent moment of inertia
T_o	Transmml:mitted torque of the AMT output shaft
ω_o	AMT output shaft's speed
i_g	AMT's gear ratio ($\frac{\omega_i}{\omega_o}$) determined by the gear position
η_g	AMT's transmission efficiency
T_f	Resistance torque of the AMT output shaft

The dynamic equation of the AMT driving dynamic model can be expressed as Equation (6).

$$M\dot{X} + CX = F \tag{6}$$

where M is mass matrix expressed as $M = \begin{bmatrix} J_i & \\ & J_o \end{bmatrix}$, X is speed matrix expressed as $X = [\omega_i\ \omega_o]^T$, C is damping matrix expressed as $C = \begin{bmatrix} C_i & \\ & C_o \end{bmatrix}$, and F is force matrix expressed as $F = \begin{bmatrix} T_i - \frac{T_o}{i_g \eta_g} \\ T_o - T_f \end{bmatrix}$.

The transmitted torque of the AMT input shaft is the transmitting torque of the clutch, which can be expressed as a third-order polynomial concerning the big end displacement of the diaphragm spring [32,33]. In this way, the motor torque is determined by the clutch control. Based on the lever principle, the clutch actuator can control its displacement to control the big end displacement of the diaphragm spring. Thus, the clutch transmitting torque can also be expressed as a third-order polynomial concerning the displacement of the clutch actuator, which can be expressed as Equation (7).

$$T_i = \mu' \left[K_1(x - x_0) + K_2(x - x_0)^2 + K_3(x - x_0)^3 \right] \tag{7}$$

where μ' is the friction coefficient of the clutch disk, x is the displacement of the clutch actuator, and x_0 is the displacement of the clutch actuator at the critical point for beginning to transmit torque.

Based on the above Equations (6) and (7), the dynamic equation of the AMT output shaft can be expressed as Equation (8).

$$\begin{cases} J_o \dot{\omega}_o + C_o \omega_o = T_o - T_f \\ T_o = T_i i_g \eta_g - J_i i_g^2 \eta_g \dot{\omega}_o - C_i i_g^2 \eta_g \omega_o \\ T_i = \mu' \left[K_1(x - x_0) + K_2(x - x_0)^2 + K_3(x - x_0)^3 \right] \end{cases} \tag{8}$$

The discrete dynamic equation of the AMT output shaft can be expressed as Equation (9) according to Equation (8).

$$\begin{cases} J_o \dot{\omega}_o(k) + C_o \omega_o(k) = T_o(k) - T_f(k) \\ \dot{\omega}_o(k) = \frac{1}{T}(\omega_o(k) - \omega_o(k-1)) \\ T_o(k) = T_i(k) i_g \eta_g - J_i i_g^2 \eta_g \dot{\omega}_o(k) - C_i i_g^2 \eta_g \omega_o(k) \\ T_i(k) = \mu' \left[K_1(x(k) - x_0) + K_2(x(k) - x_0)^2 + K_3(x(k) - x_0)^3 \right] \end{cases} \tag{9}$$

where T is the sampling interval, $\dot{\omega}_o(k)$ is the AMT output shaft's angular acceleration at k sampling time, $\omega_o(k)$ and $\omega_o(k-1)$ are the AMT output shaft's angular speed at k sampling time and $k-1$ sampling time, $T_i(k)$ is the transmitted torque of the AMT input shaft, $T_o(k)$ is the transmitted torque of the AMT output shaft, $T_f(k)$ is the resistance torque of the AMT output shaft, and $x(k)$ is the displacement of the clutch actuator at k sampling time.

3.3. Belt Conveyor Model

A belt conveyor is composed of a head pulley (driving pulley), tail pulley, tensioning pulley, bend pulley, upward roller, and downward roller. The belt conveyor model is shown in Figure 5. The whole conveyor belt can be tightened by applying tensioning force at the tensioning pulley. F_t is the tensioning force at the tensioning pulley. Tensions of the tight edge and the loose edge are F_1 and F_2, respectively; the driving force at the driving pulley is F_d.

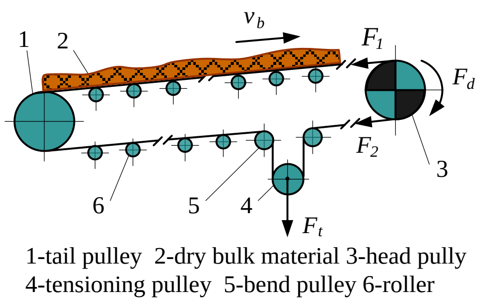

Figure 5. Belt conveyor model.

The relationship between the driving force, the tight tensioning force, and the loose tensioning is expressed as Equation (10).

$$F_d = F_1 - F_2 \tag{10}$$

where F_d is driving force at the driving pulley.

The relationship between the tight tensioning force and the loose tensioning force is analyzed as below if the belt is about to slip. Regarding the belt contacting the head pulley as the research object, taking a micro belt length dl for the purpose of force analysis, the tensions of the micro belt length are analyzed as shown in Figure 6. dF_N is the compressing force of head pulley acting on the belt, μ is the friction coefficient, μdF_N is the friction force between the belt and the driving pulley, $d\alpha$ is the corresponding belt contact angle for the micro belt length dl, α is the belt wrap angle between the belt and the driving pulley, and F and $F + dF$ are the tensioning forces at both sides of micro belt length dl.

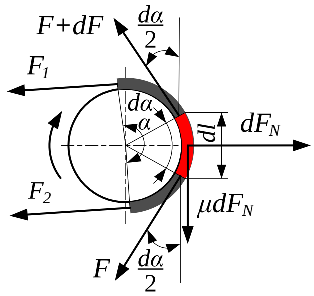

Figure 6. Tension analysis for belt drive.

The dynamic equation of micro belt length dl can be expressed as Equation (11) if the belt is about to slip.

$$\begin{cases} \mu dF_N = (F + dF)cos\frac{d\alpha}{2} - Fcos\frac{d\alpha}{2} \\ dF_N = (F + dF)sin\frac{d\alpha}{2} + Fsin\frac{d\alpha}{2} \end{cases} \tag{11}$$

Supposing that $d\alpha$ is a small wrap angle, $sin\frac{d\alpha}{2}$ and $cos\frac{d\alpha}{2}$ are similar to $\frac{d\alpha}{2}$ and 1, respectively, under the infinitesimal transformation method; the value of $dFsin\frac{d\alpha}{2}$ is a high-order infinitesimal which is similar to 0. Then, Equation (12) can be obtained.

$$\begin{cases} \frac{dF}{F} = \mu d\alpha \\ \int_{F_2}^{F_1} \frac{dF}{F} = \int_0^{\alpha} \mu d\alpha \end{cases} \tag{12}$$

Based on Equation (12), the relationship between the tight tensioning force and the loose tensioning force is expressed as Equation (13) if the belt is about to slip.

$$F_1 = F_2 e^{\mu\alpha} \tag{13}$$

where $e^{\mu\alpha}$ is the Euler coefficient.

Thus, the maximum of the effective driving force at the driving pulley is expressed as Equation (14) according to Equations (10) and (13).

$$F_{dmax} = F_1 - F_2 = F_2(e^{\mu\alpha} - 1) \tag{14}$$

In conclusion, the condition of driving and no slipping can be obtained as Equation (15).

$$F_f \leq F_d \leq F_{dmax} \tag{15}$$

where F_d is the driving force of the belt at the driving pulley and F_f is the belt resistance force.

The conveyor belt is composed of rubber, fiber, and steel core. Thus, the conveyor belt has some viscoelastic characteristics; a damp model is used to show the viscous characteristics of the conveyor belt and an elastic model is used to show the elastic characteristics of the conveyor belt. An elastic model and a damping model are connected in parallel to be represented as a Kelvin–Vogit model [34], which is used to describe the viscous and elastic characteristics of the conveyor belt. Supposing the whole belt is divided into N units, a belt unit model is built as shown in Figure 7 based on Kelvin–Vogit model.

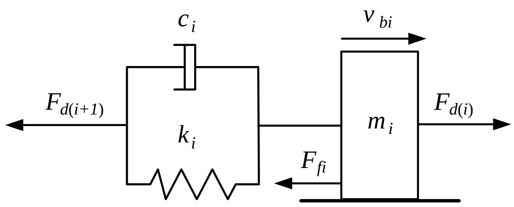

Figure 7. A belt unit model.

The dynamic equation of a belt unit model is expressed as Equation (16).

$$m_{bi}\dot{v}_{bi} + c_{bi}v_{bi} + k_{bi}x_{bi} = F_{di} - F_{d(i+1)} - F_{fi} \tag{16}$$

where m_{bi} is mass of number N unit; c_{bi} is tamping efficient of number N unit; k_{bi} is the elastic coefficient of number N unit; F_{di} and $F_{d(i+1)}$ are tensions of both ends of number N unit; F_{fi} is resistance force of number N unit; and x_{bi}, v_{bi}, and $\dot{v}_{bi}$ are belt displacement, belt speed, and belt acceleration of number N unit, respectively.

Then, the dynamic equation of the whole belt is expressed as Equation (17).

$$M\ddot{X} + C\dot{X} + KX = F \tag{17}$$

where M is mass matrix expressed as $M = \begin{bmatrix} m_{b1} & & \\ & \ddots & \\ & & m_{bN} \end{bmatrix}$, X is displacement matrix expressed as $X = [x_{b1} \ \cdots \ x_{bN}]^T$, C is damping matrix expressed as $C = \begin{bmatrix} c_{b1} & & \\ & \ddots & \\ & & c_{bN} \end{bmatrix}$, K is elastic matrix expressed as $K = \begin{bmatrix} k_{b1} & & \\ & \ddots & \\ & & k_{bN} \end{bmatrix}$, and F is force matrix expressed as $F = \left[(F_{d1} - F_{d2} - F_{f1}) \ \cdots \ \left(F_{dN} - F_{dN} - F_{fN}\right)\right]^T$.

The driving force of the belt is created from the transmitted torque of the driving pulley. The dynamic equation of the conveyor can be expressed as Equation (18).

$$\begin{cases} m_b a_b + c_b v_b + k_b x_b = F_d - F_f \\ m_b = m_{bu} + m_{bl} + m_{load} + m_p \\ F_d = \frac{T_d}{r_d} \\ T_d = T_i i_g i_r \eta_g \eta_r \\ v_b = \dot{x}_b \\ a_b = \ddot{x}_b \end{cases} \tag{18}$$

where m_b is the equivalent mass of the conveyor, a_b is the belt acceleration, v_b is the belt speed, x_b is the belt displacement, c_b is the belt damping coefficient, k_b is the belt elastic coefficient, m_{bu} is the equivalent mass of the upper belt and upper roller, m_{bl} is the equivalent mass of the lower belt and lower roller, m_{load} is the load mass on the upper belt, m_p is the equivalent mass of all pulleys, T_d is the driving torque of the driving pulley, r_d is the radius of the driving pulley, and i_r and η_r are the gear ratio and the transmission efficiency of the reducer.

Limited by the condition of driving and no slipping shown in Equation (15), the maximum value of the belt acceleration can be calculated by Equation (19) according to Equation (18).

$$a_b \leq \frac{F_{dmax} - F_f - c_b v_b - k_b x_b}{m_b} \tag{19}$$

Generally, the belt acceleration should be less than or equal to 0.3 m/s^2 for an industrial conveyor.

3.4. Segmented Angular Acceleration Curve of the AMT Output Shaft and Clutch Transmitted Torque Algorithm

Given a belt acceleration, the needed AMT output shaft's angular acceleration can be calculated from Equation (20) according to the driveline.

$$\dot{\omega}_o = \frac{a_b i_r}{r_d} \tag{20}$$

The AMT output shaft's speed can be easily tested and calculated according to the AMT output shaft's speed sensor. In addition, the AMT output shaft's angular acceleration can be calculated further. Thus, the AMT output shaft's angular acceleration can be used to control the belt acceleration. The segmented angular acceleration curve of the AMT output shaft corresponding to the segmented belt acceleration curve expressed from Equation (5) can be calculated from Equation (21).

$$\begin{cases}
\dot{\omega}_o(t) = \begin{cases} \frac{4a_{1max} i_r}{T_1 r_d} t & \left(0 \leq t \leq \frac{1}{4}T_1\right) \\ a_{1max}\frac{i_r}{r_d} & \left(\frac{1}{4}T_1 < t < \frac{3}{4}T_1\right) \\ \frac{4a_{1max} i_r}{T_1 r_d}(T_1 - t) & \left(\frac{3}{4}T_1 \leq t \leq T_1\right) \end{cases} \\
\dot{\omega}_o(t) = \begin{cases} \frac{4a_{2max} i_r}{T_2 r_d}(t - T_{s2}) & \left(T_{s2} \leq t \leq T_{s2} + \frac{1}{4}T_2\right) \\ a_{2max}\frac{i_r}{r_d} & \left(T_{s2} + \frac{1}{4}T_2 < t < T_{s2} + \frac{3}{4}T_2\right) \\ \frac{4a_{2max} i_r}{T_2 r_d}(T_{s2} + T_2 - t) & \left(T_{s2} + \frac{3}{4}T_2 \leq t \leq T_{s2} + T_2\right) \end{cases} \\
\dot{\omega}_o(t) = \begin{cases} \frac{4a_{3max} i_r}{T_3 r_d}(t - T_{s3}) & \left(T_{s3} \leq t \leq T_{s3} + \frac{1}{4}T_3\right) \\ a_{3max}\frac{i_r}{r_d} & \left(T_{s3} + \frac{1}{4}T_3 < t < T_{s3} + \frac{3}{4}T_3\right) \\ \frac{4a_{3max} i_r}{T_3 r_d}(T_{s3} + T_3 - t) & \left(T_{s3} + \frac{3}{4}T_3 \leq t \leq T_{s3} + T_3\right) \end{cases} \\
\dot{\omega}_o(t) = \begin{cases} \frac{4a_{4max} i_r}{T_4 r_d}(t - T_{s4}) & \left(T_{s4} \leq t \leq T_{s4} + \frac{1}{4}T_4\right) \\ a_{4max}\frac{i_r}{r_d} & \left(T_{s4} + \frac{1}{4}T_4 < t < T_{s4} + \frac{3}{4}T_4\right) \\ \frac{4a_{4max}}{T_4 r_d}(T_{s4} + T_4 - t) & \left(T_{s4} + \frac{3}{4}T_4 \leq t \leq T_{s4} + T_4\right) \end{cases} \\
\ldots
\end{cases} \tag{21}$$

The resistance torques of the AMT output shaft can be calculated from Equation (22).

$$T_f = \frac{T_{fd}}{i_r \eta_r} = \frac{F_f r_d}{i_r \eta_r} \tag{22}$$

where T_{fd} is the resistance torque of the head pulley.

The needed transmitted torque of the clutch can be calculated from Equation (23) according to Equation (8).

$$T_i = \frac{1}{i_g \eta_g}\left[\left(J_i i_g^2 \eta_g + J_o\right)\dot{\omega}_o + (C_i i_g^2 \eta_g + C_o)\omega_o + T_f\right] \tag{23}$$

where J_o is the AMT output shaft's equivalent moment of inertia, which can be calculated from $J_o = J_t + \frac{J_r}{i_r^2}(J_r + m_b r_d^2)$. J_t is AMT's moment of inertia at the output shaft. J_r is the reducer's moment of inertia at the output shaft.

Suppose some parameters including the load inertia and damping coefficient are invariable during the starting process. The discrete form of Equation (22) is expressed as Equation (24).

$$T_i(k) = \frac{1}{i_g \eta_g}\left[\left(J_i i_g^2 \eta_g + J_o\right)\dot{\omega}_o(k) + (C_i i_g^2 \eta_g + C_o)\omega_o(k) + T_f(k)\right] \tag{24}$$

3.5. Motor Output Torque Model

Generally, given the maximum torque and the slip ratio, the output torque of the three-phase induction motor can be expressed as Equation (25) according to the literature [35,36].

$$\begin{cases} T_m = \frac{2T_{max}}{\frac{S}{S_m} + \frac{S_m}{S}} \\ S = \frac{n_1 - n_m}{n_1} \end{cases} \tag{25}$$

where T_m is the output torque, T_{max} is the maximum torque or critical torque, s is the slip ratio, n_1 is the synchronous speed of the three-phase induction motor, n_m is the rotor speed of the three-phase induction motor, and S_m is the critical slip ratio corresponding to the maximum torque or critical torque.

4. Simulation Analysis Based on AMESim

4.1. Simulation Model and Parameter Setting

To show the dynamic response of soft-starting system based on the designed soft-starting acceleration curve for belt conveyor, a simulation model based on AMESim software using AMT as the soft starter for the belt conveyor with 300 kW is built as shown in Figure 8.

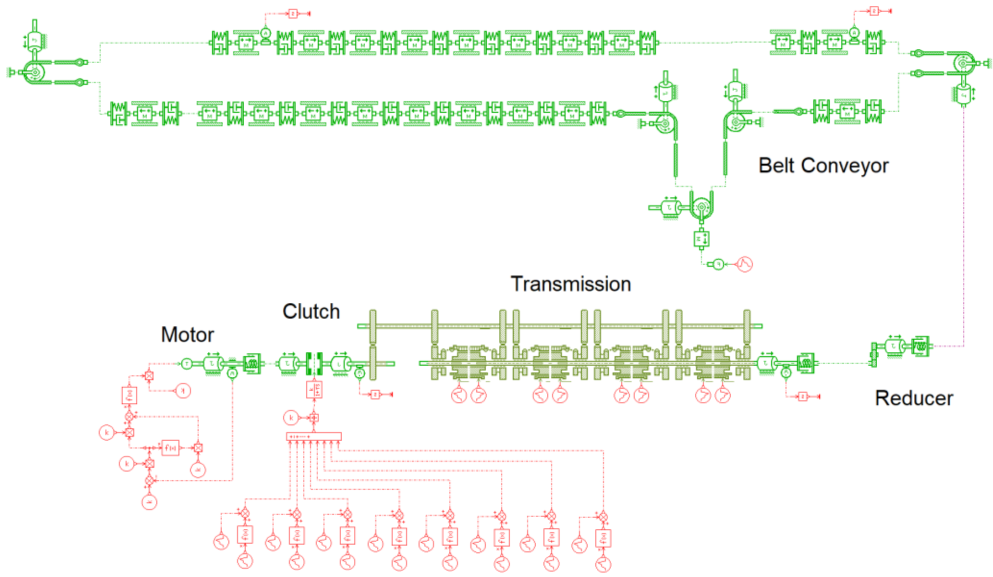

Figure 8. Simulation model based on AMESim.

The belt conveyor is built according to Equations (10), (16), and (17) from Section 3.3. The upper and lower belts are divided into 10 parts separately. AMT model is composed of two parts: a clutch model and a transmission model. The model of the clutch transmitted torque is built according to Equation (23) from Section 3.4. The motor model is built according to Equation (24) from Section 3.5.

Ignoring the transmission efficiency of the driveline, the main parameters of the soft-starting system are listed in Table 2.

Table 2. Main parameters of the AMT soft-starting system.

Parameter	Unit	Value	Parameter	Unit	Value
m_b	kg	249,571	J_i	kg·m^2	0.135
r_d	m	0.5	J_t	kg·m^2	10
F_f	N	50,819	J_r	kg·m^2	31.5
C_b	N·s/m	11,928	m_{bu}	kg·	79,695
k_b	N/m	81,250	m_{bl}	kg·	57,876
C_i	N·m/rpm	5	m_{load}	kg·	109,368
F_t	N	66,540	m_p	kg·	2632
T_{max}	N·m	4456.67	i_g		14.28, 10.62, 7.87, 5.87, 4.375, 3.26, 2.43, 1.8
n_1	rpm	1500	i_r		10
C_o	N·m/rpm	5	s_m		0.0416
α	rad	π	μ		0.02

Given the motor's rated speed of 1485 rpm, the designed belt speeds from first to eighth gear positions are 0.54, 0.73, 0.99, 1.32, 1.78, 2.38, 3.20, and 4.32 m/s, respectively. Correspondingly, the AMT output shaft's speeds from first to eighth gear positions are 103.99, 139.83, 188.69, 252.98, 339.43, 455.52, 611.11, and 825.00 rpm, respectively.

Limited by the belt's maximum acceleration of 0.3 m/s^2, the belt's designed maximum acceleration according to the segmented acceleration curve is designed to be less than 0.2 m/s^2 under different gear positions in this paper. Therefore, the acceleration stage times for every gear position are 4, 4, 4, 4, 6, 6, 8, and 10 s successively. After the acceleration stage for the first gear position is finished, the run time is 5 s. The run time is 3 s after the acceleration stage under other gear positions.

Owing to the needs of shifting and accelerating, clutch disengaging, shifting to neutral gear, choosing gear, shifting to a higher gear, and clutch engaging should operate successively. The time for clutch disengaging is 0.2 s, including 0.1 s for transmitting torque and 0.1 s for no torque. The time for shifting to neutral gear is 0.1 s. The time for choosing gear is 0.1 s. The time for shifting to a higher gear is 0.2 s. The time for clutch engaging before belt accelerating is 0.3 s, including 0.1 s for no torque (to eliminate the gap between the release bearing and the diaphragm small end) and 0.2 s for transmitting torque up to a half-engagement point. The time for clutch engaging during the belt accelerating stage is determined by the segmented acceleration curve for the gear position.

4.2. Simulation Results

Based on the above parameters, a simulation of the soft-starting process for a belt conveyor with 300 kW was conducted. To show the characteristics of the belt, the conveyor, and the AMT during the soft-starting process, some parameter variation curves are given below. The print interval of the simulation results is 0.01 s. Figures 9–11 show the speed, acceleration, and jerk of the upper belt, respectively. Figure 12 shows the belt tensions of the upper belt. Figure 13 shows the tensions of the driving pulley of the conveyor. Figure 14 shows the speed, acceleration, and jerk of the AMT output shaft.

By shifting from first to eighth gear and acceleration control, the belt speed increases to the target speed of 4.32 m/s gradually, as shown in Figure 9a. The belt speed decreases because of larger load inertia during the clutch disengaging for shifting. By comparison, the belt speed of the rear part lags behind that of the front part in Figure 9b, which explains the belt viscoelasticity. Therefore, several seconds are needed to make the whole belt run to ensure that the rear part of the belt reaches the target speed after the front part of the belt reaches the target speed under every gear position of the AMT.

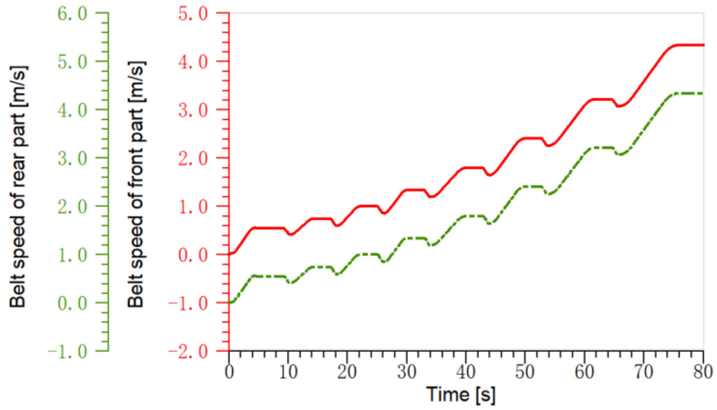

(**a**) Whole soft-starting process from first gear to eighth gear

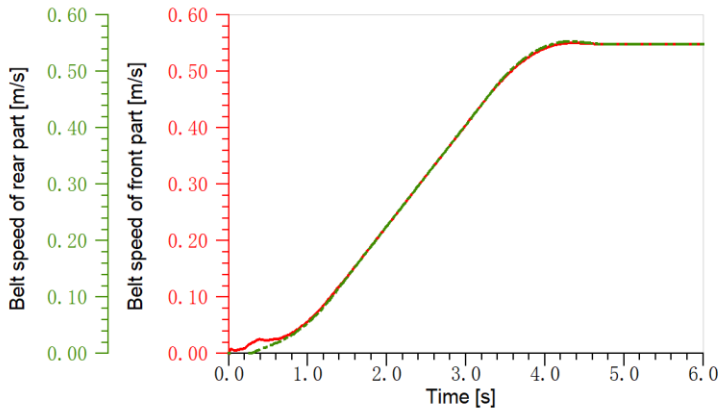

(**b**) Beginning stage under first gear

Figure 9. Belt speed curve.

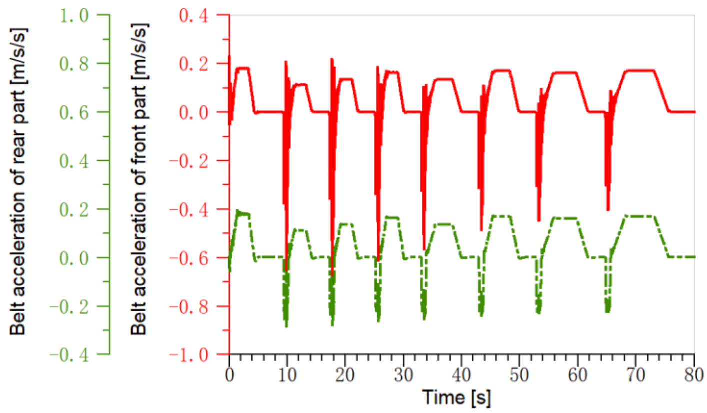

(**a**) Whole soft-starting process from first gear to eighth gear

Figure 10. *Cont.*

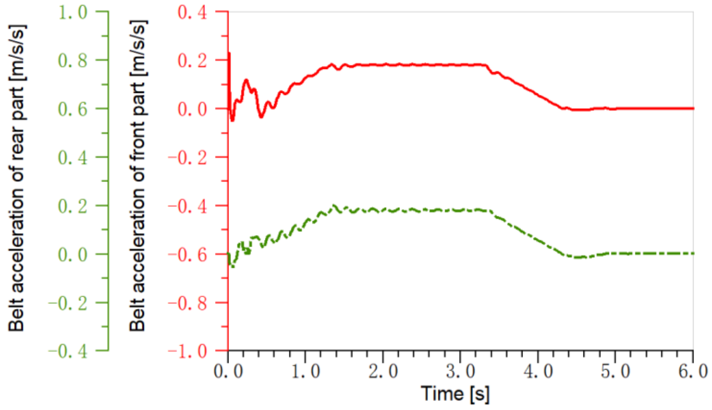

(**b**) Beginning stage under first gear

Figure 10. Belt acceleration curve.

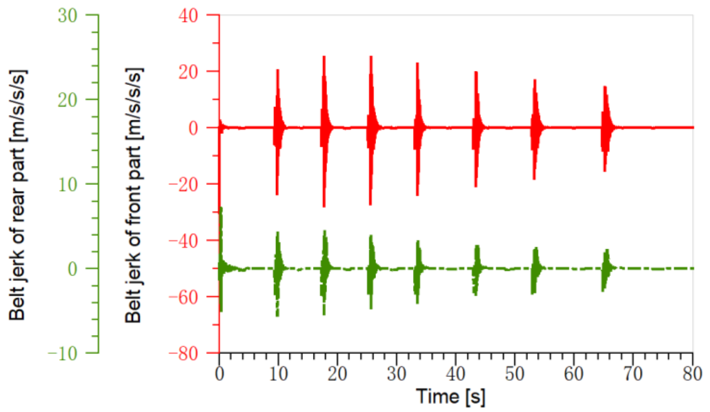

(**a**) Whole soft-starting process from first gear to eighth gear

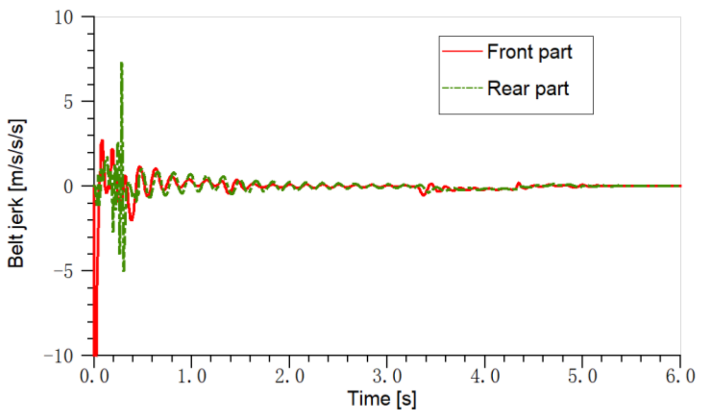

(**b**) Beginning stage under first gear

Figure 11. Belt jerk curve.

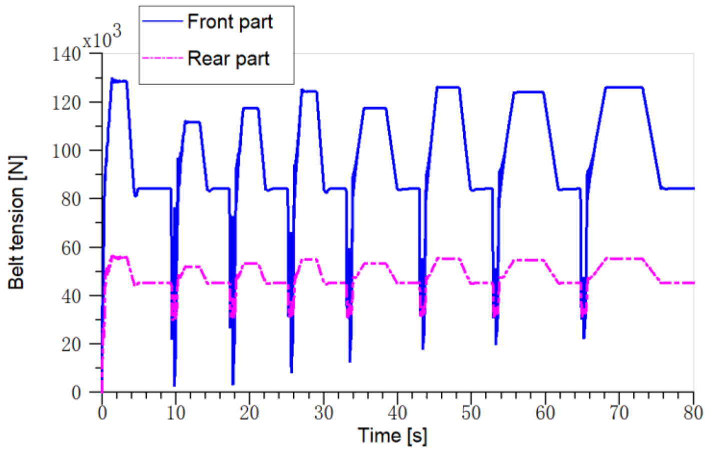

Figure 12. Belt tension curve.

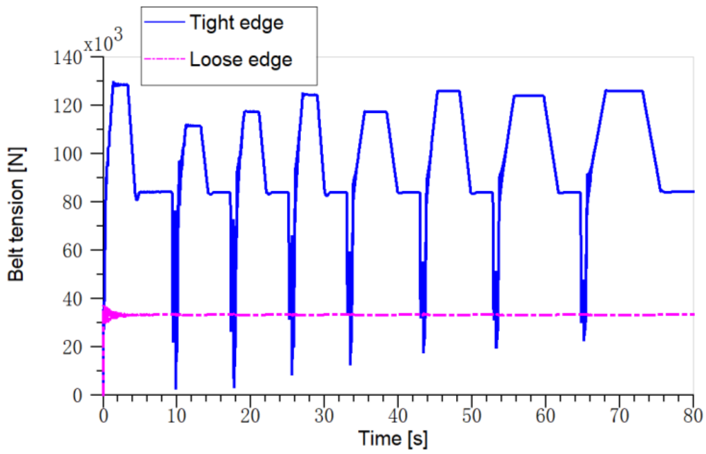

Figure 13. Belt tension curve of the driving pulley.

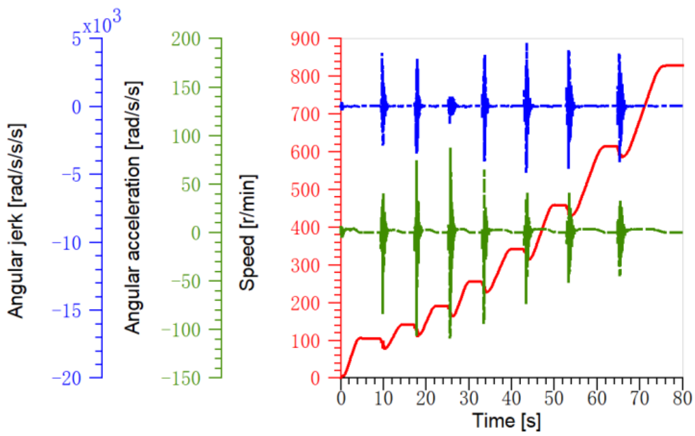

Figure 14. Parameter variation curve of the AMT's output shaft.

The belt acceleration curve from first to eighth gear is shown in Figure 10a. The belt maximum acceleration of every gear position is less than 0.2 m/s^2, which meets the requirements of soft starting. The belt acceleration vibrates because of the belt resistance force during the clutch disengaging for shifting. Basically, the belt is accelerated according to the designed segmented acceleration curve. Obviously, the vibration of the front part is not stronger than that of the rear part. The belt acceleration curve at the beginning stage of soft starting is quite consistent with the designed segmented acceleration curve in Figure 10b. With the starting of the front part, the rear belt follows.

The belt jerk curve from first to eighth gear is shown in Figure 11a, which shows that the belt jerk during the belt accelerating stage is quite smaller than that during the clutch disengaging. The belt jerk changes with the belt acceleration. The belt maximum jerk of the front part is obviously greater than that of the rear part during the clutch disengaging under the influence of the driveline. The belt maximum jerk is 0.337 m/s^3 at the moment of 22.15 s during the belt accelerating process except for the time of power interruption because of shifting. The belt jerk curve at the beginning of soft starting is shown in Figure 11b, which shows that the belt jerk of the rear part changes with that of the front part.

The belt tension curve from first to eighth gear is shown in Figure 12. The belt maximum tension of the front part is given to drive the whole belt; the maximum value is 130,086 N during the first gear position corresponding to the belt acceleration curve. The belt maximum tension of the rear part is only 56,739 N during the first gear position. The belt tensions of the front and rear parts are 84,033 N and 45,124 N, respectively. The tension difference between the front and rear parts is needed to overcome the belt resistance force of the upper belt.

The belt tension curve of the driving pulley from first to eighth gear is shown in Figure 13. The belt tension of the tight edge varies with the belt acceleration curve derived from the transmitted torque of the driving pulley. The belt tension of the loose edge changes little because the loose edge of the driving pulley is near the tensioning pulley. The belt tensions of the tight and loose edges are 84,033 N and 33,214 N, respectively, after the acceleration stage is finished under the eighth gear position.

The AMT output shaft's speed, angular acceleration, and angular jerk curves during the whole soft-starting process from first to eighth gear are shown in Figure 14. The AMT output shaft's speed increases with the increasing of the gear position gradually, which is consistent with the belt speed. It reaches the speed of 827.06 r/min, which is determined by the motor speed and the transmission ratio of the eighth gear position. The AMT output shaft's angular acceleration curve changes almost in line with the designed segmented acceleration curve if the power interruption is ignored. That is to say, the belt acceleration can be controlled by controlling the AMT output shaft's angular acceleration determined by the clutch transmitted torque. The AMT output shaft's maximum angular jerk is 215.06 rad/s^3 at the moment of 30.04 s.

By comparing the speed curves and the acceleration curves between the belt and the AMT output shaft, it can be seen that their shapes are similar, which shows that controlling the AMT output shaft's accelerating process will control the belt accelerating process. The soft-starting process of the belt conveyor can be shown from front to rear parts; the parameters curves of the whole belt, including the belt speed, belt acceleration, and belt jerk, are clearly manifested.

5. Conclusions

In this paper, a new segmented acceleration curve is proposed as the soft-starting acceleration curve for belt conveyors based on AMT. The belt speed is increased by shifting and accelerating until the speed reaches the target designed speed. The modeling of the AMT soft-starting system is built, including the AMT driving modeling and the belt conveyor modeling. The AMT output shaft's angular acceleration can be taken as the control parameter to control the belt acceleration because the AMT output shaft's speed and angular acceleration can be obtained and calculated from the AMT output shaft's speed sensor. In the environment of AMESim, the AMT soft-starting system simulation model was built, and the simulation results of the acceleration process from first to eighth gear position have been given. The results prove that the belt's moving has a lag phenomenon and the segmented acceleration curve is reasonable for the belt's acceleration process in terms of the belt's viscoelastic characteristics. Except for the power interruption time of clutch disengaging for shifting, the belt acceleration and the AMT output shaft's angular acceleration curves are in line with the designed segmented acceleration curve. The paper provides a theoretical and feasible solution for AMT to further research on the soft-starting process of the medium-scale belt conveyors.

Author Contributions: Conceptualization, Y.L.; methodology, Y.L.; software, Y.L.; validation, L.L.; formal analysis, Y.L.; investigation, L.L.; resources, Y.L.; data curation, Y.L.; writing—original draft preparation, Y.L.; writing—review and editing, Y.L.; visualization, L.L.; supervision, Y.L.; project administration, Y.L.; funding acquisition, L.L. All authors have read and agreed to the published version of the manuscript.

Funding: This research was funded by Key R & D Project of Shandong Province, China, grant number 2020CXGC11003.

Institutional Review Board Statement: Not applicable.

Informed Consent Statement: Not applicable.

Data Availability Statement: Data sharing not applicable.

Acknowledgments: This work was supported by Key R&D Project of Shandong Province, China (Grant No. 2020CXGC011003).

Conflicts of Interest: The authors declare no conflict of interest.

References

1. Grzesiek, A.; Zimroz, R.; Sliwinski, P.; Gomolla, N.; Wylomanska, A. Long term belt conveyor gearbox temperature data analysis-statistical tests for anomaly detection. *Measurement* **2020**, *165*, 108124. [CrossRef]
2. Hou, C.; Qiao, T.; Zhang, H.; Pang, Y.; Xiong, X. Multispectral visual detection method for conveyor belt longitudinal tear. *Measurement* **2019**, *143*, 246–257. [CrossRef]
3. Lozier, M.S. Deconstructing the conveyor belt. *Science* **2010**, *328*, 1507–1511. [CrossRef]
4. Wang, G.; Zhang, L.; Sun, H.; Zhu, C. Longitudinal tear detection of conveyor belt under uneven light based on haar-adaBoost and cascade algorithm. *Measurement* **2021**, *168*, 108341. [CrossRef]
5. Yang, R.; Qiao, T.; Pang, Y.; Yang, Y.; Zhang, H.; Yan, G. Infrared spectrum analysis method for detection and early warning of longitudinal tear of mine conveyor belt. *Measurement* **2020**, *165*, 107856. [CrossRef]
6. He, D.; Pang, Y.; Lodewijks, G. Green operations of belt conveyors by means of speed control. *Appl. Energy* **2017**, *188*, 330–341. [CrossRef]
7. He, D.; Pang, Y.; Lodewijks, G. Speed control of belt conveyors during transient operation. *Powder Technol.* **2016**, *301*, 622–631. [CrossRef]
8. He, D.; Liu, X.; Zhong, B. Sustainable belt conveyor operation by active speed control. *Measurement* **2020**, *154*, 107458. [CrossRef]
9. Ji, J.; Miao, C.; Li, X. Cosine-trapezoidal soft-starting control strategy for a belt conveyor. *Math. Probl. Eng.* **2019**, *2019*, 8164247. [CrossRef]
10. Bebic, M.Z.; Ristic, L.B. Speed controlled belt conveyors: Drives and mechanical considerations. *Adv. Electr. Comput. Eng.* **2018**, *18*, 51–60. [CrossRef]
11. Czubak, P.; Lis, A. Analysis of a new vibratory conveyor allowing for a sudden stopping of the transport. *Teh. Vjesn.-Tech. Gaz.* **2020**, *27*, 520–526.
12. He, D.; Pang, Y.; Lodewijks, G.; Liu, X. Healthy speed control of belt conveyors on conveying bulk materials. *Powder Technol.* **2018**, *327*, 408–419. [CrossRef]
13. Yao, Y.; Zhang, B. Influence of the elastic modulus of a conveyor belt on the power allocation of multi-drive conveyors. *PLoS ONE* **2020**, *15*, E0235768. [CrossRef] [PubMed]
14. Meng, Q.; Hou, Y. Effect of oil film squeezing on hydro-viscous drive speed regulating start. *Tribol. Int.* **2010**, *43*, 2134–2138.
15. Li, L.; Cui, H.; Lian, Z.; Wang, Q. Modeling and optimization of soft start-up for hydroviscous drive applied to scraper Conveyor. *Math. Probl. Eng.* **2019**, *2019*, 6131364. [CrossRef]
16. Myklebust, A.; Eriksson, L. Modeling, observability, and estimation of thermal effects and aging on transmitted torque in a heavy duty truck with a dry clutch. *IEEE-ASME Trans. Mechatron.* **2015**, *20*, 61–72. [CrossRef]
17. Gao, B.; Lu, X.; Chen, H.; Lu, X.; Li, J. Dynamics and control of gear upshift in automated manual transmissions. *Int. J. Veh. Des.* **2013**, *63*, 61–83. [CrossRef]
18. Gao, B.; Chen, H.; Ma, Y.; Sanada, K. Design of nonlinear shaft torque observer for trucks with Automated Manual Transmission. *Mechatronics* **2011**, *21*, 1034–1042. [CrossRef]
19. Li, Y.; Wang, Z. Motion characteristics of a clutch actuator for heavy-duty vehicles with automated mechanical transmission. *Actuators* **2021**, *10*, 179. [CrossRef]

20. Li, Y.; Li, L. Parameter estimation of a countershaft brake for heavy-duty vehicles with automated mechanical transmission. *Processes* **2021**, *9*, 1036. [CrossRef]
21. Hofman, T.; Ebbesen, S.; Guzzella, L. Topology optimization for hybrid electric vehicles with automated transmissions. *IEEE Trans. Veh. Technol.* **2012**, *61*, 2442–2451. [CrossRef]
22. Gao, B.; Chen, H.; Liu, Q.; Chu, H. Position control of electric clutch actuator using a triple-step nonlinear method. *IEEE Trans. Ind. Electron.* **2014**, *61*, 6995–7003. [CrossRef]
23. Li, Y.; Wang, Z.; Cong, X. Constant acceleration control for AMT's application in belt conveyor's soft starting. *Int. J. Control Autom.* **2013**, *6*, 315–326. [CrossRef]
24. Li, Y.; Lu, Y.; Sun, H.; Yan, P. Study on load parameters estimation during AMT startup. *J. Control Sci. Eng.* **2018**, *2018*, 7391968. [CrossRef]
25. Harrison, A. Belt conveyor research 1980–2000. *Bulk Solids Handl.* **2001**, *21*, 159–164.
26. Harrison, A.; Roberts, A.W. Technical requirements for operating conveyor belts at high speed. *Bulk Solid Handl.* **1984**, *4*, 99–104.
27. Nordell, L.K.; Ciozada, Z.P. Transient belt stresses during starting and stopping: Elastic response simulated by finite element method. *Bulk Solid Handl.* **1984**, *4*, 93–98.
28. Lodewijks, G. Non-linear dynamics of belt conveyor systems. *Bulk Solids Handl.* **1997**, *17*, 57–67.
29. Singh, M.P. Role of drive system technology in maximizing the performance and economics of long belt conveyors. *Bulk Solids Handl.* **1994**, *14*, 695–702.
30. Song, W.; Deng, Y.; Peng, Z. Simulation of the starting process of belt conveyor. *J. Northeast. Univ. (Nat. Sci.)* **1998**, *19*, 312–315.
31. Bardos, A. Starting ramps of overland (long distance) belt conveyors. *Bulk Solids Handl.* **2000**, *20*, 153–157.
32. Yan, Z.; Yan, F.; Liang, J.; Duan, Y. Detailed modeling and experimental assessments of automotive dry clutch engagement. *IEEE Access* **2019**, *7*, 59100–59113. [CrossRef]
33. Li, L.; Wang, X.; Qi, X.; Li, X.; Cao, D.; Zhu, Z. Automatic cutch control based on estimation of resistance torque for AMT. *IEEE-ASME Trans. Mechatron.* **2016**, *21*, 2682–2693. [CrossRef]
34. Li, J.; Pang, X. Belt conveyor dynamic characteristics and influential factors. *Shock Vib.* **2018**, *2018*, 8106879. [CrossRef]
35. Li, Y.; He, B.; Yuan, P.; Nie, R.; Li, G. Variable frequency drive and transmission system of the heavy armoured face conveyor. *China J. Mech. Eng.* **2018**, *54*, 8–17. [CrossRef]
36. Nie, R.; He, B.; Yuan, P.; Zhang, L.; Li, G. Novel approach to and implementation of design and analysis of armored face conveyor power train. *Sci.-China-Technol. Sci.* **2015**, *58*, 2153–2168. [CrossRef]